Bioorganic & Medicinal Chemistry 18 (2010) 8035–8043

Contents lists available at ScienceDirect

Bioorganic & Medicinal Chemistry

journal homepage: www.elsevier.com/locate/bmc

# Design, synthesis and bioevaluation of dihydropyrazolo[3,4-*b*]pyridine and benzo[4,5]imidazo[1,2-*a*]pyrimidine compounds as dual KSP and Aurora-A kinase inhibitors for anti-cancer agents

Rong-geng Fu [a,b], Qi-dong You [a,b,*], Lei Yang [c], Wu-tong Wu [d], Cheng Jiang [a,b], Xiao-li Xu [a,b]

[a] *Jiangsu Key Laboratory of Carcinogenesis and Intervention, China Pharmaceutical University, 24 Tongjiaxiang, Nanjing 210009, PR China*
[b] *Department of Medicinal Chemistry, China Pharmaceutical University, 24 Tongjiaxiang, Nanjing 210009, PR China*
[c] *Department of Natural Medicinal Chemistry, China Pharmaceutical University, 24 Tongjiaxiang, Nanjing 210009, PR China*
[d] *School of Life Science and Technology, China Pharmaceutical University, 24 Tongjiaxiang, Nanjing 210009, PR China*

ARTICLE INFO

*Article history:*
Received 10 July 2010
Revised 6 September 2010
Accepted 8 September 2010
Available online 16 September 2010

*Keywords:*
Kinesin spindle protein inhibitor
Aurora-A
Kinase inhibition
Dihydropyrazolo[3,4-*b*]pyridine
Benzo[4,5]imidazo[1,2-*a*]pyrimidine
Anticancer

ABSTRACT

Four series of dihydropyrazolo[3,4-*b*]pyridines and benzo[4,5]imidazo[1,2-*a*]pyrimidines were designed and synthesized as dual KSP and Aurora-A kinase inhibitors for anti-cancer agents by introducing some fragments of Aurora-A kinase inhibitors into our KSP inhibitor CPUYL064. A total of 19 target compounds were evaluated by two related enzyme inhibition assays and a cytotoxicity assay in vitro. The results showed that some target compounds could inhibit both enzymes, and several of them showed significant inhibition activity against HCT116 cell line. Despite showing moderate KSP and Aurora-A kinase inhibition, the lead compounds **6a** and **6e** displayed significant cytotoxic activity in the micromolar range, especially against the HCT116 cell line and HepG2 cell line. The results may be useful for developing a new class of inhibitors having a dual function, KSP inhibition and Aurora-A kinase inhibition, for the treatment of cancer.

© 2010 Elsevier Ltd. All rights reserved.

## 1. Introduction

Uncontrolled proliferation in cancer cells is dependent upon mitosis and its related processes. Therefore, a proven effective strategy in cancer treatment has been to interfere with abnormal progression of mitosis in order to halt the cell cycle in mitosis and to induce apoptosis in tumor cells. Recently, much attention has been focused on the new mitotic targets including the polo-like kinases (PLKs), Aurora kinases, and kinesin motor proteins.

Kinesin spindle protein, known as KSP or Hs Eg5, has recently emerged as a key target for selective antimitotic cancer therapy. KSP is uniquely expressed in dividing cells, and its motor activity has been shown to be required early in mitosis for the establishment of a functional, bipolar mitotic spindle.[1] So far no role for KSP outside mitosis has been found. A range of structurally diverse KSP inhibitors have been shown to cause cell cycle arrest, differentiation and/or apoptosis of tumor cells. During the past 10 years, the first generation of KSP inhibitors, including monastrol,[2] ispinesib,[3] CK0106023[4] and ARRY-520[5] have been reported, and several of these are now undergoing clinical trials.[6] Monastrol (Fig. 1) is the first specific KSP inhibitor shown to be noncompetitive with microtubule (MT), and acting through an allosteric site. In order to find potential KSP inhibitors, our group recently reported a novel kind of KSP inhibitors by rational drug design. Among them, CPUYL064 (Fig. 1) was found to be more potent than monastrol in both KSP ATPase inhibitory and the ability to anti-proliferation of human hepatocellular liver carcinoma cell line HepG2.[7]

On the other hand, Aurora kinases (Aurora-A, Aurora-B, and Aurora-C) are vital component playing a critical role in regulating many of the processes that are pivotal to mitosis, and they are required for healthy cell growth and proliferation. It was reported that Aurora-A kinase are overexpressed in a broad range of tumor cell lines and human primary tumors; thus, the inhibition of Aurora-A kinase, by small molecules is becoming an area of major current interest in oncology drug discovery.[8] These discovery efforts have led to several lead compounds (e.g., compound **1a**[9] and **1b**[10]) and clinical candidates (e.g., VX-680[11]) (Fig. 1). VX-680 was the first inhibitor of Aurora kinases and entered clinical trials. Analysis of the crystal structure of Abl/VX-680 complexes reveals that the aminomethylpyrazole group in VX-680 is anchored to the hinge with three ATP-type hydrogen bonds.[12] The conserved H-bonding interactions of inhibitors with hinge region residues are observed in most of the inhibitor-Aurora complex structures and are essential for maintaining activity.[8]

Considering KSP and Aurora A kinase are two key enzymes in the mitotic machinery,[13] and KSP is one of Aurora A kinase substrates, we proposed to design a new kind of dual inhibitors by combining

* Corresponding author. Tel.: +86 25 83271351.
*E-mail addresses:* youqd@cpu.edu.cn, youqidong@gmail.com (Q. You).

0968-0896/$ - see front matter © 2010 Elsevier Ltd. All rights reserved.
doi:10.1016/j.bmc.2010.09.020

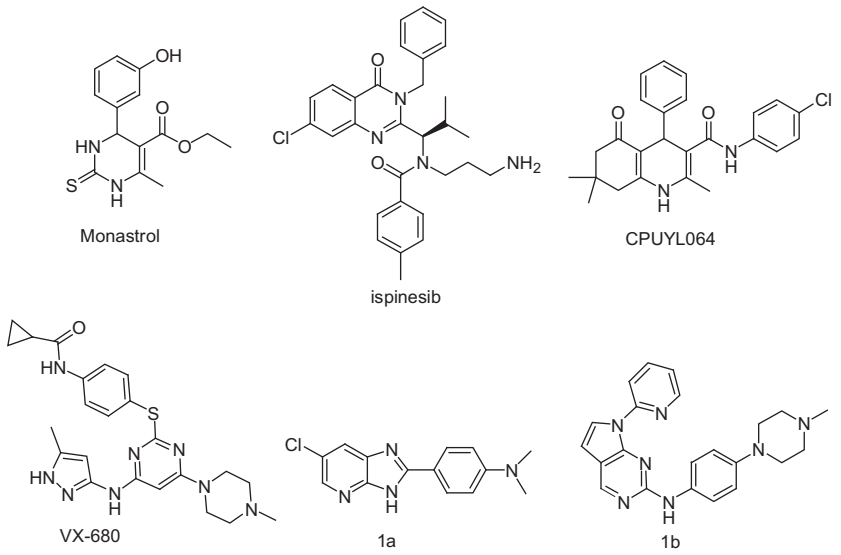


**Figure 1.** Structure of KSP and Aurora kinase inhibitors.

KSP inhibitor's scaffold with Aurora-A kinase inhibitor's fragment. The dual targets of KSP and Aurora-A kinase may be more effective for blocking multiple key components of the mitotic machinery compared to separate agents and would be beneficial to enhance antitumor activity toward a wide range of cancers. With the goal of identifying such a new anti-cancer strategy, we devised a strategy to derivatize CPUYL064 in such a way so as to facilitate its binding to Aurora-A kinase while maintaining its KSP inhibitory activity.

Based on the pharmacophore we have identified and the binding mode analysis for KSP inhibitors,[14,15] we mapped the structure of CPUYL064 with the pharmacophore of KSP inhibitor, which consists of four chemical features (Fig. 2): one aromatic ring (part 1), one hydrophobic group (part 2), a side chain (part 3) and a flexible heterocyclic ring (part 4). Substituted pyrazoles are common feature of Aurora-A kinase inhibitor scaffolds which formatted three ATP-type hydrogen bonds to hinge residues.[8] In order to incorporating Aurora-A kinase inhibitory functionality into the scaffold of the KSP, our strategy is to utilize dihydropyrazolo[3,4-*b*]pyridine moiety as the core structure in which the pyrazole ring was supposed to perform as a hinge region-interacting group while the dihydropyridine ring maintained in CPUYL064 as a KSP scaffold. Thus, the structure of CPUYL064 was modified by replacing the dihydropyridine group with dihydropyrazolo[3,4-*b*]pyridine moiety and altering the benzene ring with different heterocyclic systems to afford three series of target compounds (series 1–3). Some compounds demonstrated significant KSP inhibitory activities along with modest Aurora-A kinase inhibition. To optimize further and determine the optimal hinge region-interacting group, we carried out a more extensive exploration of this site by replacing the pyrazole group with the benzimidazole moiety to afford the target compounds (series 4), which utilized benzo[4,5]imidazo[1,2-*a*]pyrimidine moiety as the core structure.

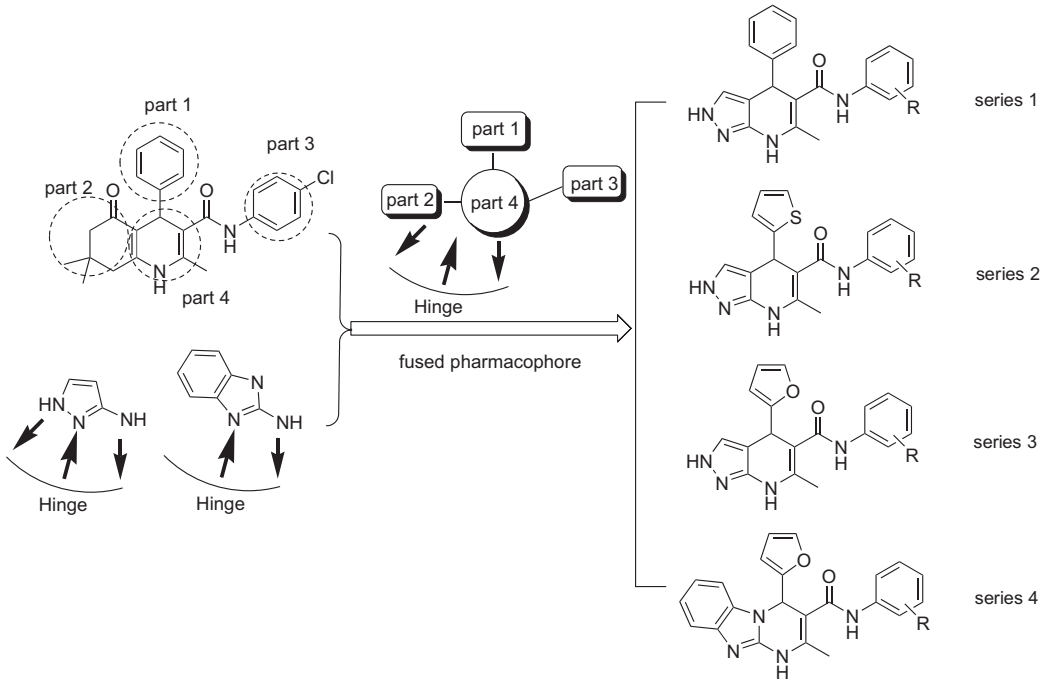


**Figure 2.** The design of the dual inhibitors of KSP and Aurora-A kinase.

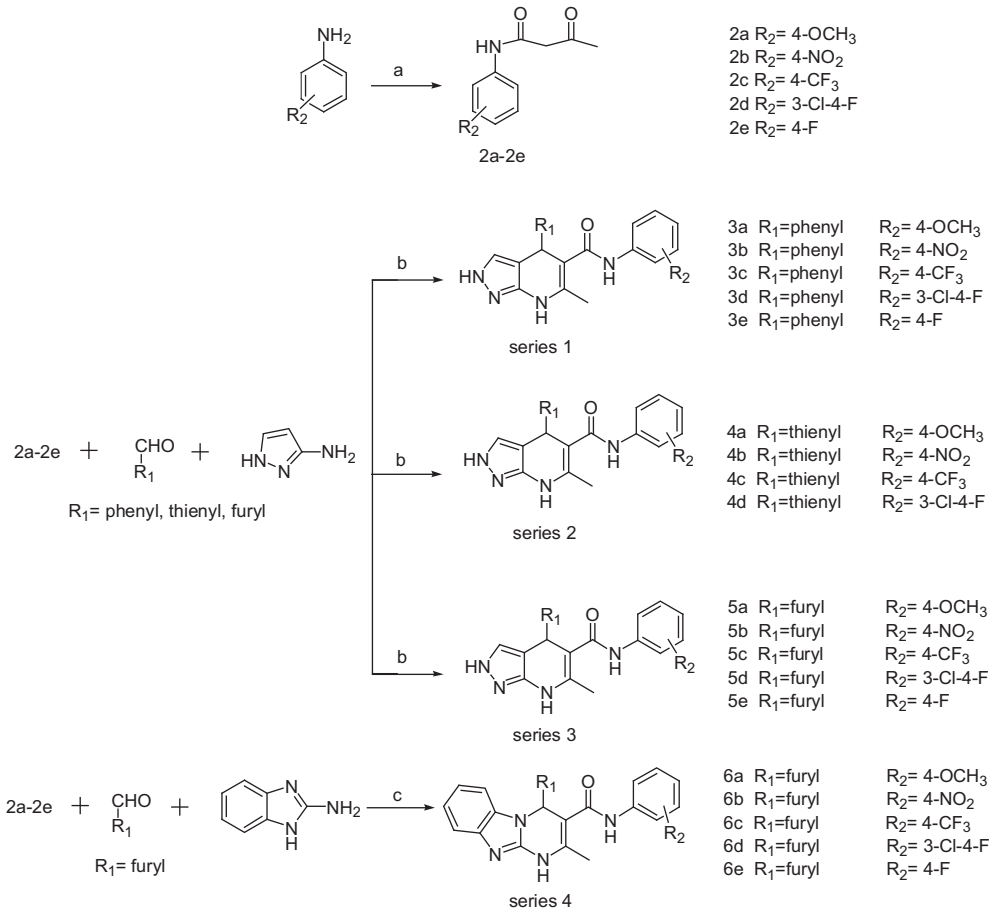


**Scheme 1.** General route for the synthesis of dihydropyrazolo[3,4-*b*]pyridines. Reagents and conditions: (a) $CH_3COCH_2COOC_2H_5$, toluene, 10 h, reflex; (b) $FeCl_3$, $C_2H_5OH$, 1–3 h, 50 °C; (c) CAN, $C_2H_5OH$, 1–3 h, 50 °C.

## 2. Chemistry

The synthesis of the dihydropyrazolo[3,4-*b*]pyridines (**3a**–**3e**, **4a**–**4d** and **5a**–**5e**) is presented in Scheme 1. *N*-Alkyl acetylacetamides **2a**–**2e** were prepared by ester/amide exchange reaction. The one-pot reaction involves a three-component condensation reaction of 3(5)-aminepyrazole, *N*-alkyl acetylacetamides **2a**–**2e** and the appropriate aromatic aldehyde in the presence of $FeCl_3$ as a catalyst at ambient temperature.

Several methods are available for the synthesis of benzo[4,5]imidazo[1,2-*a*]pyrimidines.[16,17] Despite related reactions utilizing various β-dicarbonyl compounds have been reported by several groups, our investigation represents the precursors of the use of *N*-alkyl-3-oxobutanamide and ceric ammonium nitrate (CAN) as catalyst in this process. Compounds (**6a**–**6e**) were prepared according to the procedures described in Scheme 1. In a typical experiment, 2-aminobenzimidazole, *N*-alkyl acetylacetamides, 2-furaldehyde and ceric ammonium nitrate were dissolved in absolute ethanol. The reaction mixture was maintained for 1–3 h at ambient temperature followed by removal of the solvent under vacuum and subsequent purification by recrystallization from ethanol to yield the product (**6a**–**6e**). The benzo[4,5]imidazo[1,2-*a*]pyrimidines and dihydropyrazolo[3,4-*b*]pyridines were all synthesized as racemic mixtures.

## 3. Results and discussion

KSP inhibitory activity was assessed by measuring the release of inorganic phosphate from ATP hydrolysis through absorbance detection of a malachite green-phosphate complex.[18] The $IC_{50}$ values of the target compounds against KSP were determined by measuring the activities of microtubule-activated ATPase activity. Monastrol, CPUYL064 and CK0106023 were synthesized[19,20] and used as positive controls. In order to obtain potential compounds with specific inhibitory effect against Aurora-A kinase, we used the Aurora-A kinase activity assay kit developed by Cell Signaling Technology. Compound **1a** was synthesized[21] and used as positive controls. The anti-proliferative cytotoxic activity was also evaluated by using HCT116 tumor cell line.

The data in Table 1 clearly showed that all dihydropyrazolo[3,4-*b*]pyridine compounds exhibited significant inhibiting activities toward KSP with the $IC_{50}$ values range in the domains of 0.001–10.4 μM. Given the $IC_{50}$ for CPUYL064 is 0.18 μM, the introduction of the pyrazole Aurora-A inhibiting pharmacophore at the dihydropyridine is comparably tolerated but gradually decreases KSP inhibitory in these three series of dihydropyrazolo[3,4-*b*]pyridines. With the exception of compounds **3d**, **3e**, **4a** and **5a**, all the other dihydropyrazolo[3,4-*b*]pyridines were weaker than CPUYL064, generally inhibiting KSP at nanomolar to low micromolar levels. The highest activity was observed for compound **5a**, with $IC_{50}$ of 1.1 nM, while **5e** being the lowest with 10.36 μM. The phenyl-substituted compound **3a** inhibited the KSP activity at concentrations up to 2.82 μM, while the other compounds **3b**–**3e** demonstrated more potent inhibitory effects than the corresponding thienyl or furyl-substituted compounds, with the $IC_{50}$ values in the submicromolar range (from 0.14 to 0.4 μM). Generally, when the $R_1$ group was furyl or thienyl, the $IC_{50}$ values increased with the electrophilic group or halogen substitution and decreased with

**Table 1**
Bioactivity and lipophilicity of the synthesized dihydropyrazolo[3,4-*b*]pyridines

| Compound | $R_2$ | KSP $IC_{50}$[a] (μM) | Aurora-A $IC_{50}$ (μM) | mi log *P*[b] | HCT116 $IC_{50}$[c] (μM) |
|---|---|---|---|---|---|
| **3a** | 4-$OCH_3$ | 2.82 | >50 | 3.456 | >50 |
| **3b** | 4-$NO_2$ | 0.20 | >50 | 3.358 | 33.76 |
| **3c** | 4-$CF_3$ | 0.40 | >50 | 4.294 | 4.97 |
| **3d** | 3-Cl-4-F | 0.17 | >50 | 4.169 | 2.36 |
| **3e** | 4-F | 0.14 | >50 | 3.563 | 42.68 |
| **4a** | 4-$OCH_3$ | 0.0025 | >50 | 3.355 | >50 |
| **4b** | 4-$NO_2$ | 0.82 | >50 | 3.257 | 21.02 |
| **4c** | 4-$CF_3$ | 0.32 | >50 | 4.193 | 11.56 |
| **4d** | 3-Cl-4-F | 0.44 | >50 | 4.068 | 25.00 |
| **5a** | 4-$OCH_3$ | 0.0011 | 9.25 | 2.713 | >50 |
| **5b** | 4-$NO_2$ | 2.76 | >50 | 2.615 | >50 |
| **5c** | 4-$CF_3$ | 1.06 | >50 | 3.552 | >50 |
| **5d** | 3-Cl-4-F | 0.40 | 15.00 | 3.426 | 19.76 |
| **5e** | 4-F | 10.36 | 8.10 | 2.820 | 39.79 |
| Monastrol | / | 5.47 | >50 | 2.409 | >50 |
| CPUYL064 | / | 0.18 | 40.34 | 5.746 | 12.70 |
| CK0106023 | / | 0.029 | >50 | 5.943 | 0.94 |
| **1a** | / | 40.18 | 4.97 | 3.572 | 4.71 |

[a] The inhibitory activities against KSP were determined by measuring the MT-activated ATPase activity.
[b] Lipophilicity was evaluated by in silico calculation developed at Molinspiration. Calculation was performed using Molinspiration online property calculation toolkit (http://www.molinspiration.com).
[c] $IC_{50}$ values were derived from single dose–response curves generated from triplicate data points.

the incorporation of the methoxy group at the side chain $R_2$ group. These results suggest that the substituent groups of $R_1$ play an important role with regard to KSP inhibitory. And more clearly, the phenyl or thienyl series are generally preferred for the inhibition of KSP.

For Aurora-A kinase, the inhibition activities of the dihydropyrazolo[3,4-*b*]pyridines were relatively weak compared with that against KSP. The changed $R_1$ group of these three series compounds affected the inhibition activity towards Aurora-A kinase. When the $R_1$ group was phenyl and thienyl, compounds **3a**–**3e** and **4a**–**4d** resulted in a substantial loss in potency for Aurora-A kinase. However it was interesting that compounds **5a**, **5d** and **5e** with the $R_1$ group being furyl showed better inhibition activities against Aurora-A kinase with the $IC_{50}$ values of 9.25, 15.00 and 8.10 μM, respectively, compared with the phenyl and thienyl substituted compounds. The introduction of phenyl and thienyl at $R_1$ group cause significant potency loss in Aurora-A kinase inhibitory, presumably due to unfavorable steric interactions affecting the binding motif of the molecule in the Aurora-A kinase hinge site. These results indicate that the furyl substituent on the $R_1$ group proved to be important for Aurora-A kinase inhibition in these dihydropyrazolo[3,4-*b*]pyridines.

All the dihydropyrazolo[3,4-*b*]pyridines were evaluated for cytotoxicity to cancer HCT116 cell line by means of the 3-(4,5-dimethylthiazol-2-yl)-2,5-diphenyl tetrazolium bromide (MTT) assay as described elsewhere.[22] As shown in Table 1, these three series of dihydropyrazolo[3,4-*b*]pyridine compounds were mostly only moderately to weakly potent growth inhibition of HCT116 cell line, while compound **3c** and **3d** was found to have more potency against HCT116 cell line with the $IC_{50}$ values of 4.97 and 2.36 μM, respectively, compared with that of the positive control CPUYL064's 12.70 μM. Compounds with thienyl group at the $R_1$ group, such as **4b**, **4c** and **4d**, showed moderate anti-proliferative cytotoxic activities with an $IC_{50}$ in the 11–25 μM range. At enzymatic level compounds **3a**–**3e** and **4a**–**4d** showed more potent inhibition of KSP than Aurora-A kinase. Thus, the potential effect of Aurora-A kinase inhibition on proliferation of HCT116 cells may be negligible. The furyl derivatives **5a**–**5e** also showed some anti-proliferation activities in the preliminary screening, but their $IC_{50}$ values were all less potent than 10 μM. It has been observed from Table 1 that most of the dihydropyrazolo[3,4-*b*]pyridines with halogen substituent groups at the side chain $R_2$ group such as 3-chloro-4-fluoro especially, have significantly higher cytotoxicities than those with electron contributing groups or electron-withdrawing groups. Compound **5a** exhibited the most potent inhibitory activity for KSP and moderate activity for Aurora-A kinase; however, the cytotoxicity dramatically decreased. The expanded discrepancy might be come from the poor lipophilicity of the compounds. In addition to the anti-cancer activity, the relationships between the cytotoxic effects on HCT116 cells (shown by the $IC_{50}$ values) and the lipophilicity (shown by mi log *P* values[23]) of these three series compounds were determined and shown in Table 1. The mi log *P* values for these three series compounds are in the range 2.6–4.3. The compounds with mi log *P* values between 4.0 and 4.3 were more active for HCT116 cancer cells. The cytotoxicity gradually rise with increasing the lipophilicity caused by the introduction of different halogen substituents at $R_2$ group. Evidenced by the lower mi log *P* value that indicates lipophilicity for those compounds such as **5a**, we proposed that the disappointing cytotoxicities of those compounds could be attributed to the relatively poor membrane permeability of them. By increasing lipophilicity of these three series compounds, we could expect an increase in the affinity of the compounds for the lipid bilayer of the cell membrane and thus an easier penetration into the cell.

From our structure–activity relationship (SAR) studies as discussed above, it can be concluded that the phenyl or thienyl series are generally preferred for the inhibition of KSP whereas furyl series leads to potent inhibition of Aurora-A kinase. To optimize further and determine the optimal hinge region-interacting group, we align the scaffold of compound **5e** to the known Aurora-A kinase inhibitor **1b**. The molecular alignment of compounds **1b** and **5e** is shown in Figure 3. With the aim of increasing hydrophobic interaction with the hinge region of the Aurora kinase and retaining the global shape of **5e**, we kept the furyl substituent on the $R_1$ group and replaced the pyrazole group with the benzimidazole moiety to afford compounds **6a**–**6e**.

As shown in Table 2, it was observed that replacement of the pyrazole group by the benzimidazole moiety for compounds **5a**–**5e** leads to enhancement of the inhibitory kinase activity for Aurora-A. Unlike Aurora-A kinase inhibition, the benzo[4,5]imidazo[1,2-*a*]pyrimidine derivatives (compounds **6a**–**6e**) decreases some potency of KSP inhibition. Although compounds **6a**–**6e** were moderately potent KSP and Aurora-A kinase inhibitory fused-molecules, most compounds displayed more balanced inhibitory activities against two targets compare to dihydropyrazolo[3,4-*b*]pyridines and showed more potent anti-proliferative activities against the HCT116 cell line with $IC_{50}$ ranging from 4.9 to 11.5 μM, which were comparable to the positive control CPUYL064. Compound **6a** exhibited significantly inhibition on the growth of the HCT116 cells, much more active than its counterpart compound **5a**. Correspondingly, mi log *P* value for compound **6a** (mi log *P* = 4.177) was higher than for compounds **5a** (mi log *P* = 2.713) indicating better membrane penetration which could at least partially account for the good cytotoxicity obtained despite weaker KSP inhibition and similar Aurora-A kinase inhibition. Compounds **6b** and **6d** show similar inhibitory activity against Aurora-A kinase and similar anti-proliferative potency against HCT116 cells despite the KSP component for compound **6d**, which is nearly 20-fold higher than that of **6b**. These results indicate that the inhibition mechanisms of compounds **6b** and **6d** were mainly dominated by the inhibition of Aurora-A kinase. The low anti-proliferative activity of compound **6c** might be attributed to the poor aqueous solubility, a phenomenon that was observed in our synthetic efforts. Interestingly, compound **6e** is 30-fold less potent an inhibitor of KSP than CPUYL064 and about 1.2-fold less potent than **1a** as Aurora-A kinase inhibitor. It was

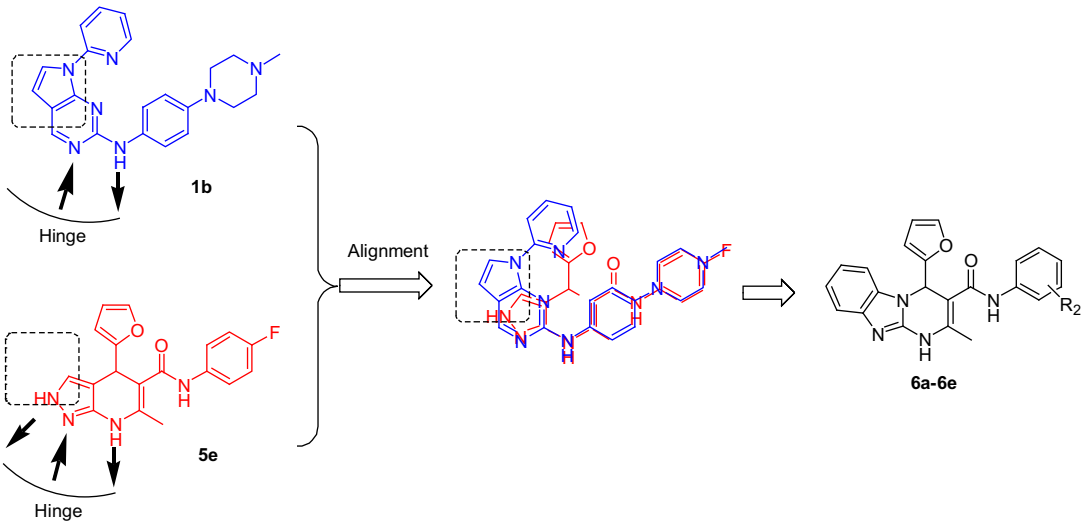


**Figure 3.** The design of the compounds **6a**–**6e**.

**Table 2**
Bioactivity and lipophilicity of the synthesized benzo[4,5]imidazo[1,2-*a*]pyrimidines

| Compound | $R_2$ | KSP $IC_{50}$[a] (μM) | Aurora-A $IC_{50}$ (μM) | mi log *P*[b] | HCT116 $IC_{50}$[c] (μM) |
|---|---|---|---|---|---|
| **6a** | 4-$OCH_3$ | 2.46 | 7.58 | 4.177 | 8.71 |
| **6b** | 4-$NO_2$ | 20.85 | 3.00 | 4.079 | 11.49 |
| **6c** | 4-$CF_3$ | 3.32 | 1.32 | 5.016 | >50 |
| **6d** | 3-Cl-4-F | 0.96 | 5.73 | 4.890 | 10.90 |
| **6e** | 4-F | 5.65 | 6.15 | 4.284 | 4.96 |
| Monastrol | / | 5.47 | >50 | 2.409 | >50 |
| CPUYL064 | / | 0.18 | 40.34 | 5.746 | 12.70 |
| CK0106023 | / | 0.029 | >50 | 5.943 | 0.94 |
| **1a** | / | 40.18 | 4.97 | 3.572 | 4.71 |

[a] The inhibitory activities against KSP were determined by measuring the MT-activated ATPase activity.
[b] Lipophilicity was evaluated by in silico calculation developed at Molinspiration. Calculation was performed using Molinspiration online property calculation toolkit (http://www.molinspiration.com).
[c] $IC_{50}$ values were derived from single dose–response curves generated from triplicate data points.

found to inhibit proliferation of HCT116 cells at a concentration ($IC_{50}$ = 4.96 μM) similar to that of **1a** ($IC_{50}$ = 4.71 μM), while compound **6e**'s anti-proliferative activity was nearly 2.5-fold higher than that of CPUYL064 ($IC_{50}$ = 12.70 μM). These results suggest that at least for compound **6e** the two components, KSP and Aurora-A kinase inhibition, both contribute to the anti-proliferative activity and the inhibition mechanism of compound **6e** was mainly dominated by the inhibition of Aurora-A kinase.

In attempts to better understand the observed SARs, docking studies with the representative compound **6e** was performed to suggest possible binding modes of the chimeras on KSP (Fig. 4) and Aurora-A kinase (Fig. 5). As shown in Figure 4, compound **6e** interacted with a cage formed by Glu116, Gly117, Glu118, Trp127, Ala133, Ile136, Pro137, Tyr211, Leu214 and Glu215, and formed one hydrogen bonds with the main chain oxygen of residue Gly117. In addition, the furan group of compound **6e** interacted with the cooperative minor pocket mainly surrounded by Arg221 and Ala218. As shown in Figure 5, the benzo[4,5]imidazo[1,2-*a*]pyrimidine core of **6e** fitted into the hinge region of Aurora-A kinase, and the benzo[4,5]imidazo[1,2-*a*]pyrimidine core *N*=C and *N*H atoms formed two H-bonds with the main chain of Ala213. In addition, the benzo[4,5]imidazo[1,2-*a*]pyrimidine core also formed hydrophobic interactions with the surrounding residues, including Leu139, Val147, Ala160, and Leu263. The large amide substituents of **6e** extend to the outer portion of the binding pocket through a region adjacent to Thr217.

Finally, the most promising compounds representing different structural series were selected for further evaluation for their anti-proliferative cytotoxic activity against other human tumor cell lines, such as HepG2 (hepatocarcinoma) and A2780 (ovarian cancer). As shown in Table 3, most tested compounds exhibited inhibitions on the growth of selected tumor cell lines, especially on HCT116 cell line. Although it was not easy to obtain an obvious structure–activity relationship from the Table 3, we could conclude that the substituent groups of the side chain play an important role with regard to cytotoxicity and the replacement of pyrazole group by the

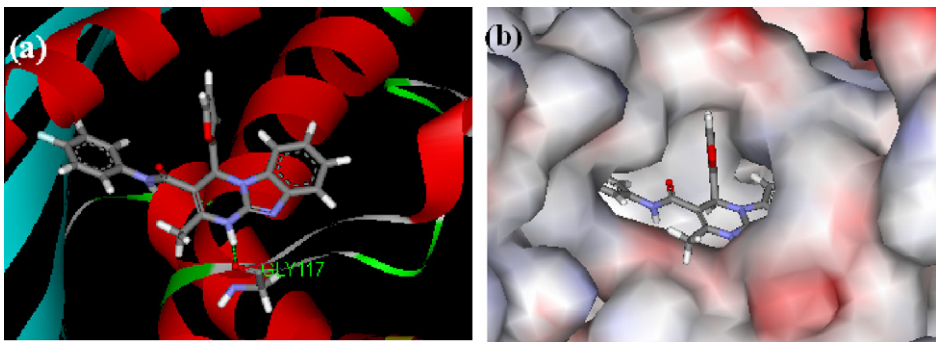


**Figure 4.** Model of compound **6e** bound to the KSP. Docking simulation was performed using the program GOLD and the crystal structure of KSP (PDB code 1Q0B). For clarity, only interacting residues are displayed. (a) Compound **6e** is depicted by sticks and balls. (b) The KSP is represented by molecular surface.

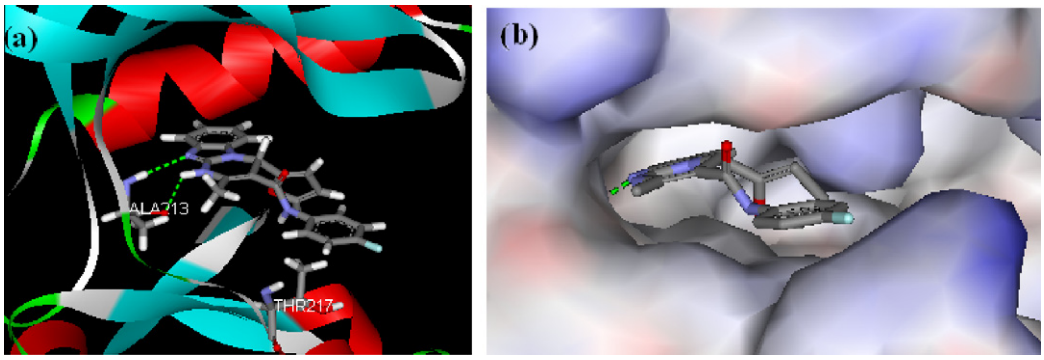


**Figure 5.** Model of compound **6e** bound to the Aurora-A kinase. Docking simulation was performed using the program GOLD and the crystal structure of Aurora-A kinase (PDB code 2BMC). For clarity, only interacting residues are displayed. (a) Compound **6e** is depicted by sticks and balls. (b) The Aurora-A kinase is represented by molecular surface.

**Table 3**
Cellular $IC_{50}$ (μM) of selected compounds

| Compound | HCT116 | A2780 | HepG2 |
|---|---|---|---|
| **3c** | 4.97 | >50 | 29.40 |
| **3d** | 2.36 | 20.00 | 42.38 |
| **4c** | 11.56 | 10.12 | >50 |
| **5d** | 19.76 | 48.49 | >50 |
| **6a** | 8.71 | 9.34 | 4.97 |
| **6b** | 11.49 | 3.05 | 13.54 |
| **6d** | 10.90 | >50 | 25.98 |
| **6e** | 4.96 | >50 | 7.38 |
| CK0106023 | 0.94 | 3.00 | 2.10 |
| **1a** | 4.71 | 4.26 | 5.85 |

benzimidazole moiety for compounds **5a**–**5e** leads to an increased cytotoxicity to the human tumor cell lines. Compound **6a** exhibited good anti-proliferative cytotoxicity against several tumor cell lines. Specifically, it had an $IC_{50}$ value of 4.97 μM against human hepatocellular liver carcinoma cell line HepG2, and this was similar to the anti-proliferative cytotoxicity of CK0106023 and compound **6e** with an $IC_{50}$ value of 2.10 and 7.38 μM, respectively. Compound **6b** was found to have a similar potency against A2780 cell line with an $IC_{50}$ value of 3.05 μM compared with that of CK0106023's 3.00 μM. Further evaluation of benzo[4,5]imidazo[1,2-*a*]pyrimidine compound's anti-cancer mechanism was on the way.

## 4. Conclusions

The correlation between KSP inhibition and suppression of tumor growth has brought the design of KSP inhibitors to the forefront of cancer research and is validated as an important cancer target. By combining structural features from known inhibitors of KSP and Aurora-A, we have been able to design, synthesize and evaluate two types of dual inhibitors of KSP and Aurora-A based on a CPUYL064 core structure. Although, compounds **6a** and **6e** identified through this new design approach were moderately potent KSP and Aurora-A kinase inhibitory fused-molecules, these two compounds displayed significant cytotoxic activity in the micromolar range, especially against the HCT116 cell line and HepG2 cell line. Taken together these results suggest that the compounds described in this study can serve as lead analogs for further development of more potent dual KSP and Aurora-A inhibitors in single molecules.

## 5. Experimental

### 5.1. General

Melting points were determined on a Mel-TEMP II melting point apparatus and are uncorrected. Infrared (IR) spectra (KBr) were recorded on a Nicolet Impact 410 instrument (KBr pellet). $^1$H NMR spectra were recorded with a Bruker Avance 300 MHz spectrometer at 300 K, using TMS as an internal standard. MS spectra were recorded on a Shimadzu GC–MS 2010 (EI) or a Mariner Mass Spectrum (ESI), or a LC/MSD TOF HRMS Spectrum. All compounds were routinely checked by TLC and $^1$H NMR. TLCs and preparative thin-layer chromatography were performed on silica gel GF/UV 254, and the chromatograms were performed on silica gel (200–300 mesh) visualized under UV light at 254 and 365 nm. All solvents were reagent grade and, when necessary, were purified and dried by standards methods. Concentration of solutions after reactions and extractions involved the use of a rotary evaporator operating at a reduced pressure of ca. 20 Torr. Organic solutions were dried over anhydrous sodium sulfate. Analytical results are within (0.50% of the theoretical values).

### 5.2. General procedure for the synthesis of compounds 2a–2e

Ethyl acetoacetate (40 mmol) and aniline (40 mmol) was dissolved in toluene (100 mL) under nitrogen atmosphere. The mixture was stirred at refluxing for 10 h, then remove of the major part of solvent in vacuo. The mixture was concentrated and purified by column chromatography on silica gel by eluting with a mixture of petroleum ether/ethyl acetate (1:2) to give the desired product.

#### 5.2.1. *N*-(4-Methoxyphenyl)acetylacetamide (2a)

Yield 16.6%, white powdery crystal, mp 112–114 °C. $^1$H NMR (300 MHz, $CDCl_3$): $\delta$ 2.33 (s, 3H), 3.58 (s, 2H), 3.79 (s, 3H), 6.86 (d, 2H, $J$ = 9.0 Hz), 7.44 (d, 2H, $J$ = 9.0 Hz), 8.93 (s, 1H). EI-MS (*m*/*z*): 207 ($M^+$).

#### 5.2.2. *N*-(4-Nitrophenyl)acetylacetamide (2b)

Yield 76.1%, yellow powdery crystal, mp 103–106 °C. $^1$H NMR (300 MHz, $CDCl_3$): $\delta$ 2.40 (s, 3H), 3.65 (s, 2H), 7.48 (d, 2H, $J$ = 9.0 Hz), 8.22 (d, 2H, $J$ = 9.0 Hz), 9.75 (s, 1H). EI-MS (*m*/*z*): 222 ($M^+$).

#### 5.2.3. *N*-(4-Trifluoromethylphenyl)acetylacetamide (2c)

Yield 36.1%, white powdery crystal, mp 92–95 °C. $^1$H NMR (300 MHz, $CDCl_3$): $\delta$ 2.35 (s, 3H), 3.63 (s, 2H), 7.58 (d, 2H, $J$ = 8.4 Hz), 7.69 (d, 2H, $J$ = 8.7 Hz), 9.46 (s, 1H). EI-MS (*m*/*z*): 245 ($M^+$).

#### 5.2.4. *N*-(3-Chloro-4-fluorophenyl)acetylacetamide (2d)

Yield 62.3%, white powdery crystal, mp 65–66 °C. $^1$H NMR (300 MHz, $CDCl_3$): $\delta$ 3.34 (s, 3H), 3.60 (s, 2H), 7.08 (t, 1H, $J$ = 9.0 Hz), 7.44 (m, 1H), 7.75 (m, 1H), 9.33 (s, 1H). EI-MS (*m*/*z*): 229 ($M^+$).

#### 5.2.5. *N*-(4-Fluorophenyl)acetylacetamide (2e)

Yield 62.3%, white powdery crystal, mp 98–100 °C. $^1$H NMR (300 MHz, $CDCl_3$): $\delta$ 2.33 (s, 3H), 3.59 (s, 2H), 7.02 (t, 2H, $J$ = 8.4 Hz), 7.51 (m, 2H), 9.15 (s, 1H). EI-MS ($m/z$): 195 ($M^+$).

### 5.3. General procedure for the synthesis of compounds 3a–3e, 4a–4d and 5a–5e

A solution of 5-aminopyrazole (1.2 mmol), *N*-alkyl-3-oxobutanamides (1.2 mmol) and aldehyde (1.2 mmol) in absolute ethanol (5 mL) was heated to 50 °C with stirring under nitrogen atmosphere. After stirred for 60 min, the mixture was added a catalytic amount of ferric chloride. The precipitation was occurred in 60–180 min, filtrated to yield the crude product, which was purified by recrystallization from 95% EtOH to give the desired compounds.

#### 5.3.1. 4-Phenyl-6-methyl-*N*-(4-methoxyphenyl)-4,7-dihydro-2*H*-pyrazole[3,4-*b*]pyridine-5-carboxamide (3a)

Yield 30%, mp 155–157 °C. IR (cm$^{-1}$): 3411, 3292, 1643, 1598, 1510. $^1$H NMR (300 MHz, DMSO-$d_6$): $\delta$ 2.11 (s, 3H), 3.67 (s, 3H), 5.32 (s, 1H), 6.77 (d, 2H, $J$ = 8.7 Hz), 7.07 (m, 1H), 7.15–7.22 (m, 5H), 7.47 (d, 2H, $J$ = 9.0 Hz), 8.62 (s, 1H), 9.15 (s, 1H), 11.81 (s, 1H). EI-MS ($m/z$): 360 ($M^+$). HRMS (ESI): Calcd for ($C_{21}H_{20}N_4O_2$)-$Na^+$: 383.1484. Found: 383.1467 [M+Na]$^+$.

#### 5.3.2. 4-Phenyl-6-methyl-*N*-(4-nitrophenyl)-4,7-dihydro-2*H*-pyrazole[3,4-*b*]pyridine-5-carboxamide (3b)

Yield 15.5%, mp 224–226 °C. IR (cm$^{-1}$): 3414, 3293, 3195, 1644, 1598, 1510, 1408, 1242, 1172, 1031, 826, 785. $^1$H NMR (300 MHz, DMSO-$d_6$): $\delta$ 2.17 (s, 3H), 5.42 (s, 1H), 7.20–7.21 (m, 6H), 7.75 (d, 2H, $J$ = 9.0 Hz), 8.10 (d, 2H, $J$ = 9.0 Hz), 9.00 (s, 1H), 9.87 (s, 1H), 11.92 (s, 1H). EI-MS ($m/z$): 375 ($M^+$). HRMS (ESI): Calcd for ($C_{20}H_{17}N_5O_3$)$Na^+$: 398.1229. Found: 398.1226 [M+Na]$^+$.

#### 5.3.3. 4-Phenyl-6-methyl-*N*-(4-trifluoromethylphenyl)-4,7-dihydro-2*H*-pyrazole[3,4-*b*]pyridine-5-carboxamide (3c)

Yield 27%, mp 259–260 °C. IR (cm$^{-1}$): 3401, 3315, 3198, 3081, 1644, 1598, 1523, 1403, 1332, 1254, 1111, 1064, 827, 705. $^1$H NMR (300 MHz, DMSO-$d_6$): $\delta$ 2.15 (s, 3H), 5.40 (s, 1H), 7.07 (m, 1H), 7.20–7.22 (m, 5H), 7.55 (d, 2H, $J$ = 8.7 Hz), 7.68 (d, 2H, $J$ = 8.1 Hz), 8.87 (s, 1H), 9.63 (s, 1H), 11.89 (s, 1H). EI-MS ($m/z$): 398 ($M^+$). HRMS (ESI): Calcd for ($C_{21}H_{17}F_3N_4O$)$Na^+$: 421.1252. Found: 421.1269 [M+Na]$^+$.

#### 5.3.4. 4-Phenyl-6-methyl-*N*-(3-chloro-4-fluorophenyl)-4,7-dihydro-2*H*-pyrazole[3,4-*b*]pyridine-5-carboxamide (3d)

Yield 23%, mp 222–224 °C. IR (cm$^{-1}$): 3401, 3308, 3201, 3084, 1641, 1500, 1391, 1251, 1149, 1073, 808, 701. $^1$H NMR (300 MHz, DMSO-$d_6$): $\delta$ 2.14 (s, 3H), 5.36 (s, 1H), 7.08 (m, 1H), 7.18–7.28 (m, 6H), 7.40 (m, 1H), 7.80 (m, 1H), 8.81 (s, 1H), 9.48 (s, 1H), 11.87 (s, 1H). EI-MS ($m/z$): 382 ($M^+$). HRMS (ESI): Calcd for ($C_{20}H_{16}ClFN_4O$)$H^+$: 383.1077. Found: 383.1070 [M+H]$^+$.

#### 5.3.5. 4-Phenyl-6-methyl-*N*-(4-fluorophenyl)-4,7-dihydro-2*H*-pyrazole[3,4-*b*]pyridine-5-carboxamide (3e)

Yield 25%, mp 232–234 °C. IR (cm$^{-1}$): 3404, 3301, 3084, 2360, 1642, 1600, 1509, 1400, 1221, 1149, 820, 702. $^1$H NMR (300 MHz, DMSO-$d_6$): $\delta$ 2.12 (s, 3H), 5.34 (s, 1H), 7.02–7.25 (m, 8H), 7.48 (d, 1H, $J$ = 2.1 Hz), 7.50 (d, 1H, $J$ = 2.1 Hz), 8.68 (s, 1H), 9.31 (s, 1H), 11.85 (s, 1H). EI-MS ($m/z$): 348 ($M^+$). EI-MS ($m/z$): 348 ($M^+$). HRMS (ESI): Calcd for ($C_{20}H_{17}FN_4O$)$H^+$: 349.1466. Found: 349.1455 [M+H]$^+$.

#### 5.3.6. 4-Thiophene-6-methyl-*N*-(4-methoxyphenyl)-4,7-dihydro-2H-pyrazole[3,4-*b*]pyridine-5-carboxamide (4a)

Yield 56%, mp 223–225 °C. IR (cm$^{-1}$): 3385, 3318, 1640, 1602, 1514, 1405, 1317, 1244, 1132, 1030, 826, 723. $^1$H NMR (300 MHz, DMSO-$d_6$): $\delta$ 2.09 (s, 3H), 3.69 (s, 3H), 5.67 (s, 1H), 6.80 (m, 4H), 7.20 (d, 1H), 7.43 (s, 1H), 7.45 (d, 2H, $J$ = 8.4 Hz), 8.72 (s, 1H), 9.25 (s, 1H), 11.94 (s, 1H). EI-MS ($m/z$): 366 ($M^+$). HRMS (ESI): Calcd for ($C_{19}H_{18}N_4O_2S$)$Na^+$: 389.1048. Found: 389.1063 [M+Na]$^+$.

#### 5.3.7. 4-Thiophene-6-methyl-*N*-(4-nitrophenyl)-4,7-dihydro-2*H*-pyrazole[3,4-*b*]pyridine-5-carboxamide (4b)

Yield 19%, mp 231–233 °C. IR (cm$^{-1}$): 3377, 3298, 3080, 1638, 1525, 1496, 1343, 1252, 1158, 843, 719. $^1$H NMR (300 MHz, DMSO-$d_6$): $\delta$ 2.15 (s, 3H), 5.76 (s, 1H), 6.77–6.82 (m, 2H), 7.20 (d, 1H, $J$ = 4.8 Hz), 7.39 (s, 1H), 7.81 (d, 2H, $J$ = 9.3 Hz), 8.14 (d, 2H, $J$ = 9.3 Hz), 9.10 (s, 1H), 9.96 (s, 1H), 12.05 (s, 1H, NH). EI-MS ($m/z$): 381 ($M^+$). HRMS (ESI): Calcd for ($C_{18}H_{15}N_5O_3S$)$Na^+$: 404.0794. Found: 404.0788 [M+Na]$^+$.

#### 5.3.8. 4-Thiophene-6-methyl-*N*-(4-trifluoromethylphenyl)-4,7-dihydro-2*H*-pyrazole[3,4-*b*]pyridine-5-carboxamide (4c)

Yield 29%, mp 246–248 °C. IR (cm$^{-1}$): 3384, 3285, 3082, 1644, 1600, 1523, 1403, 1332, 1256, 1110, 1064, 829, 715. $^1$H NMR (300 MHz, DMSO-$d_6$): $\delta$ 2.13 (s, 3H), 5.73 (s, 1H), 6.78 (s, 1H), 6.81 (t, 1H, $J$ = 3.3 Hz), 7.20 (d, 1H, $J$ = 4.8 Hz), 7.37 (s, 1H), 7.58 (d, 2H, $J$ = 8.7 Hz), 7.78 (d, 2H, $J$ = 8.7 Hz), 8.95 (s, 1H), 9.72 (s, 1H), 12.00 (s, 1H). EI-MS ($m/z$): 404 ($M^+$). HRMS (ESI): Calcd for ($C_{19}H_{15}F_3N_4OS$)$Na^+$: 427.0817. Found: 427.0809 [M+Na]$^+$.

#### 5.3.9. 4-Thiophene-6-methyl-*N*-(3-chloro-4-fluorophenyl)-4,7-dihydro-2*H*-pyrazole[3,4-*b*]pyridine-5-carboxamide (4d)

Yield 45%, mp 241–243 °C. IR (cm$^{-1}$): 3390, 3275, 3198, 3083, 1640, 1600, 1500, 1388, 1243, 1132, 1054, 858, 716. $^1$H NMR (300 MHz, DMSO-$d_6$): $\delta$ 2.11 (s, 3H), 5.70 (s, 1H), 6.78 (d, 1H, $J$ = 2.7 Hz), 6.81 (t, 1H, $J$ = 3.6 Hz), 7.20 (q, 1H, $J$ = 5.1 Hz), 7.29 (t, 1H, $J$ = 9.0 Hz), 7.36 (s, 1H), 7.47 (m, 1H), 7.88 (q, 1H, $J$ = 6.9 Hz), 8.91 (s, 1H), 9.57 (s, 1H), 12.00 (s, 1H). EI-MS ($m/z$): 388 ($M^+$). HRMS (ESI): Calcd for ($C_{18}H_{14}ClFN_4OS$)$Na^+$: 411.0459. Found: 411.0466 [M+Na]$^+$.

#### 5.3.10. 4-Furan-6-methyl-*N*-(4-methoxyphenyl)-4,7-dihydro-2*H*-pyrazole[3,4-*b*]pyridine-5-carboxamide (5a)

Yield 21%, mp 261–263 °C. IR (cm$^{-1}$): 3425, 3289, 3196, 1643, 1599, 1511, 1409, 1243, 1173, 1031, 826, 734. $^1$H NMR (300 MHz, DMSO-$d_6$): $\delta$ 2.08 (s, 3H), 3.69 (s, 3H), 5.43 (s, 1H), 6.01 (d, 1H, $J$ = 3.0 Hz), 6.24 (d, 1H, $J$ = 3.0 Hz), 6.82 (d, 2H, $J$ = 9.0 Hz), 7.34 (s, 1H), 7.43 (s, 1H), 7.46 (d, 2H, $J$ = 9.0 Hz), 8.66 (s, 1H), 9.33 (s, 1H), 11.92 (s, 1H). EI-MS ($m/z$): 350 ($M^+$). HRMS (ESI): Calcd for ($C_{19}H_{18}N_4O_3$)$Na^+$: 373.1277. Found: 373.1290 [M+Na]$^+$.

#### 5.3.11. 4-Furan-6-methyl-*N*-(4-nitrophenyl)-4,7-dihydro-2*H*-pyrazole[3,4-*b*]pyridine-5-carboxamide (5b)

Yield 15%, mp 229–231 °C. IR (cm$^{-1}$): 3373, 3289, 3196, 3077, 1643, 1593, 1495, 1342, 1252, 1147, 1006, 842, 748. $^1$H NMR (300 MHz, DMSO-$d_6$): $\delta$ 2.08 (s, 3H), 5.53 (s, 1H), 5.97 (d, 1H, $J$ = 3.0 Hz), 6.24 (q, 1H, $J$ = 3.0 Hz), 7.40 (s, 1H), 7.43 (m, 1H), 7.82 (d, 2H, $J$ = 9.0 Hz), 8.15 (d, 2H, $J$ = 9.0 Hz), 9.03 (s, 1H), 10.02 (s, 1H), 12.02 (s, 1H). EI-MS ($m/z$): 365 ($M^+$). HRMS (ESI): Calcd for ($C_{18}H_{15}N_5O_4$)$Na^+$: 388.1022. Found: 388.1023 [M+Na]$^+$.

#### 5.3.12. 4-Furan-6-methyl-*N*-(4-trifluoromethylphenyl)-4,7-dihydro-2*H*-pyrazole[3,4-*b*]pyridine-5-carboxamide (5c)

Yield 17%, mp 248–250 °C. IR (cm$^{-1}$): 3388, 3293, 3084, 1649, 1602, 1524, 1403, 1332, 1257, 1111, 1008, 832, 748. $^1$H NMR (300 MHz, DMSO-$d_6$): $\delta$ 2.12 (s, 3H), 5.50 (s, 1H), 5.99 (d, 1H, $J$ = 3.0 Hz), 6.24 (q, 1H, $J$ = 3.0 Hz), 7.40 (s, 1H), 7.42 (d, 1H, $J$ = 0.9 Hz), 7.60 (d, 2H, $J$ = 8.7 Hz), 7.79 (d, 2H, $J$ = 8.7 Hz), 8.89 (s, 1H), 9.78 (s, 1H), 11.99 (s, 1H). EI-MS ($m/z$): 388 ($M^+$). HRMS

(ESI): Calcd for $(C_{19}H_{15}F_3N_4O_2)Na^+$: 411.1045. Found: 411.1051 $[M+Na]^+$.

#### 5.3.13. 4-Furan-6-methyl-*N*-(3-chloro-4-fluorophenyl)-4,7-dihydro-2*H*-pyrazole[3,4-*b*]pyridine-5-carboxamide (5d)

Yield 34%, mp 239–241 °C. IR ($cm^{-1}$): 3388, 3280, 3085, 1643, 1602, 1503, 1387, 1246, 1148, 1004, 921, 787. $^1H$ NMR (300 MHz, DMSO-$d_6$): $\delta$ 2.10 (s, 3H), 5.46 (s, 1H), 5.97 (d, 1H, $J$ = 3.0 Hz), 6.25 (q, 1H), 7.30 (t, 1H), 7.38 (s, 1H), 7.43 (d, 1H, $J$ = 0.9 Hz), 7.49 (m, 1H), 7.91 (m, 1H), 8.85 (s, 1H), 9.64 (s, 1H), 11.98 (s, 1H, NH). EI-MS ($m/z$): 372 ($M^+$). HRMS (ESI): Calcd for $(C_{18}H_{14}ClFN_4O_2)Na^+$: 395.0687. Found: 395.0697 $[M+Na]^+$.

#### 5.3.14. 4-Furan-6-methyl-*N*-(4-fluorophenyl)-4,7-dihydro-2*H*-pyrazole[3,4-*b*]pyridine-5-carboxamide (5e)

Yield 30%, mp 228–230 °C. IR ($cm^{-1}$): 3384, 3289, 3084, 1643, 1604, 1509, 1396, 1220, 1150, 1005, 823, 746. $^1H$ NMR (300 MHz, DMSO-$d_6$): $\delta$ 2.09 (s, 3H), 5.45 (s, 1H), 6.00 (d, 1H, $J$ = 3.0 Hz), 6.24 (t, 1H, $J$ = 2.7 Hz), 7.07 (t, 2H, $J$ = 9.0 Hz), 7.35 (s, 1H), 7.43 (s, 1H), 7.58 (q, 2H, $J$ = 9.0 Hz), 8.73 (s, 1H), 9.50 (s, 1H), 11.94 (s, 1H). EI-MS ($m/z$): 338 ($M^+$). HRMS (ESI): Calcd for $(C_{18}H_{15}FN_4O_2)H^+$: 339.1259. Found: 339.1268 $[M+H]^+$.

### 5.4. General procedure for the synthesis of compounds 6a–6e

A solution of 2-aminobenzimidazole (1.2 mmol), *N*-alkyl-3-oxobutanamide (1.2 mmol), 2-furaldehyde (1.2 mmol) and ceric ammonium nitrate (0.06 mmol) in absolute ethanol (2 mL) was heated to 50 °C with stirring. The precipitation was occurred in 60–180 min and the reaction mixture was cooled to room temperature. The mixture was filtered to give the crude product, which was further purified by recrystallization from 95% EtOH to give the desired compounds.

#### 5.4.1. *N*-(4-Methoxybenzyl)-4-furan-2-methyl-1,4-dihydro-benzo[4,5]imidazo[1,2-*a*]pyrimidine-3-carboxamide (6a)

Yield 35%, white powdery crystal, mp 248–250 °C (dec). IR ($cm^{-1}$): 3302, 2836, 2973, 1627, 1512, 1460, 1250. $^1H$ NMR (300 MHz, DMSO-$d_6$): $\delta$ 2.24 (s, 3H), 3.71 (s, 3H), 6.34 (s, 1H), 6.61 (s, 1H), 6.78 (s, 1H), 6.85–7.50 (m, 9H), 9.62 (s, 1H), 10.24 (s, 1H). EI-MS: ($m/z$) 400 ($M^+$). Anal. Calcd for $C_{23}H_{20}N_4O_3$: C, 68.64; H, 5.51; N, 13.92. Found: C, 68.85; H, 5.13; N, 14.07.

#### 5.4.2. *N*-(4-Nitrobenzyl)-4-furan-2-methyl-1,4-dihydro-benzo[4,5]imidazo[1,2-*a*]pyrimidine-3-carboxamide (6b)

Yield 32%, yellow powdery crystal, mp 255–256 °C (dec). IR ($cm^{-1}$): 3396, 2844, 1626, 1502, 1332, 1249. $^1H$ NMR (300 MHz, DMSO-$d_6$): $\delta$ 2.29 (s, 3H), 6.33 (s, 1H), 6.50 (s, 1H), 6.85 (s, 1H), 6.85–8.23 (m, 9H), 10.32 (s, 1H),10.50 (s, 1H). EI-MS: ($m/z$) 415 ($M^+$). Anal. Calcd for $C_{22}H_{17}N_5O_4{\cdot}0.3H_2O$: C, 62.79; H, 4.21; N, 16.64. Found: C, 62.44; H, 4.16; N, 17.14.

#### 5.4.3. *N*-(4-Trifluoromethylbenzyl)-4-furan-2-methyl-1,4-dihy dro-benzo[4,5]imidazo[1,2-*a*]pyrimidine-3-carboxamide (6c)

Yield 35%, yellow powdery crystal, mp 273–274 °C (dec). IR ($cm^{-1}$): 3290, 2850, 2360, 1629, 1522, 1407, 1331. $^1H$ NMR (300 MHz, DMSO-$d_6$): $\delta$ 2.28 (s, 3H), 6.33 (s, 1H), 6.50 (s, 1H), 6.83 (s, 1H), 6.99–7.82 (m, 9H), 10.10 (s, 1H), 10.42 (s, 1H). EI-MS: ($m/z$) 438 ($M^+$). Anal. Calcd for $C_{23}H_{17}F_3N_4O_2$: C, 63.01; H, 3.91; N, 12.78. Found: C, 62.61; H, 3.93; N, 12.88.

#### 5.4.4. *N*-(3-Chloro-4-fluorobenzyl)-4-furan-2-methyl-1,4-dihydro-benzo[4,5]imidazo[1,2-*a*]pyrimidine-3-carboxamide (6d)

Yield 30%, yellow powdery crystal, mp 273–274 °C (dec). IR ($cm^{-1}$): 3268, 2845, 1626, 1500, 1460, 1258. $^1H$ NMR (300 MHz, DMSO-$d_6$): $\delta$ 2.26 (s, 3H), 6.34 (s, 1H), 6.51 (s, 1H), 6.79 (s, 1H), 6.99–7.91 (m, 8H), 9.95 (s, 1H), 10.39 (s, 1H). EI-MS: ($m/z$) 422 ($M^+$). Anal. Calcd for $C_{22}H_{16}ClFN_4O_2$: C, 62.49; H, 3.81; N, 13.25. Found: C, 62.21; H, 3.97; N, 13.58.

#### 5.4.5. *N*-(4-Fluorobenzyl)-4-furan-2-methyl-1,4-dihydro-benzo[4,5]imidazo[1,2-*a*]pyrimidine-3-carboxamide (6e)

Yield 34%, white powdery crystal, mp 275–276 °C (dec). IR ($cm^{-1}$): 3421, 2924, 2973, 2360, 1625, 1509, 1460. $^1H$ NMR (300 MHz, DMSO-$d_6$): $\delta$ 2.05 (s, 3H), 6.34 (s, 1H), 6.52 (s, 1H), 6.79 (s, 1H), 7.01–7.60 (m, 9H), 9.83 (s, 1H), 10.33 (s, 1H). EI-MS: ($m/z$) 388 ($M^+$). Anal. Calcd for $C_{22}H_{17}FN_4O_2$: C, 68.03; H, 4.41; N, 14.43. Found: C, 67.64; H, 4.50; N, 14.36.

### 5.5. Bioactivity test

#### 5.5.1. Preparation of Eg5

Coding regions were PCR amplified from a template (obtained in our lab) containing full-length human Eg5. The primers used were, forward 5′-TATAGG GCG AAT TCC GCC ATG GCG TCG CAG CCA-3′ and reverse 5′-ACG GGC TGC AGC AAG CTC GAG TTT TAAACG TTC TAT-3′. The region encoding residues 2–386 was subcloned into pET28a (NOVAGEN). Protein expression in *Escherichia coli* cells was induced with 0.5 mM IPTG. Cells were harvested after 20 h of growth at 20 °C and then disrupted by sonication. The soluble lysate was clarified by centrifugation and applied to a SP-Sepharose column (Amersham Pharmacia Biotech) in a buffer A (20 mM Na-PIPES, pH 6.3; 20 mM NaCl; 1 mM $MgCl_2$; 1 mM Na-EGTA). Protein was eluted with a linear gradient of 20–1000 mM NaCl. Eg5 was identified by SDS–PAGE, and then applied to Mono-Q columns (Amersham Pharmacia Biotech) in a buffer B (20 mM Tris–HCl, pH 8.8; 1 mM $MgCl_2$; 1 mM Na-EGTA). A gradient from 0 to 1000 mM NaCl was used to elute Eg5. Fractions were analyzed by SDS–PAGE. The most concentrated fraction was dialyzed against ATPase buffer (20 mM Na-PIPES, pH 7.5; 1 mM $MgCl_2$; 1 mM Na-EGTA) and then aliquoted, frozen in liquid nitrogen, stored at −80 °C.

#### 5.5.2. ATPase activity assay

All experiments were done at room temperature. The reagents were added to wells of a 96-well clear plate and the final reaction of the assay contained 20 mM PIPES, pH 7.5, 5.0 mM $MgCl_2$, 1 mM EGTA, 10 mM paclitaxel, 0.6 mM tubulin (MT), 0.5 mM ATP, 2% DMSO containing inhibitors in a reaction volume of 100 mL. Reactions were started by adding ATP. The plates were incubated at 37 °C for 30 min. Following incubation the malachite-green based reagents were added to detect the release of inorganic phosphate. The plates were incubated for an additional 5 min at the room temperature, and then 34% sodium citrate of 10 mL was added. The absorbance at 610 nm was determined using Multiskan Spectrum Microplate Spectrophotometer (Thermo Electron Corporation). The controls without Eg5 or MTs are the background and should be subtracted from all values. The controls with MTs but without Eg5 give the nucleotide hydrolysis by MTs and should be subtracted from corresponding values with Eg5 and the same concentration of MTs. The data were analyzed using Microsoft Excel to obtain the $IC_{50}$ of the test compounds.

#### 5.5.3. In vitro Aurora-A kinase activity assays

To determine the inhibition of Aurora-A kinase activity by target compounds, the HTScan® Aurora-A kinase assay kit (Cell Signaling Technology) was used according to the manufacturer's instruction. Briefly, 20 ng purified recombinant human Aurora-A kinase was added to a 50 μL reaction mixture containing 1× kinase buffer and 200 μmol/L cold ATP in the presence of different concentrations of test compounds (ranging from $10^{-4}$ to $10^{-9}$ mol/L). After incubation at room temperature for 15 min, biotinylated peptide substrate (Cell Signaling Technology) was added to each reaction mixture at a final

concentration of 1.5 μmol/L, and the mixtures were further incubated for 30 min. A parallel control experiment was done under the same conditions without test compounds. The reaction was stopped by addition of 50 mmol/L EDTA (pH 8). Then, 30 μL reaction mixture was transferred to a streptavidin-coated 96-well plate (PerkinElmer, Inc.) and incubated at room temperature for 60 min. After washing thrice with PBS/T, the phosphor PLK (Ser10) antibody (Cell Signaling Technology) was added to the plate for further incubation at 37 °C for 60 min. After washing, HRP-labeled secondary antibody was added. After incubation at room temperature for 30 min, the plate was finally washed five times and the fluorescence signal was determined with BMG Polarstar Galaxy (Germany) at 450 nm. The data were analyzed using Microsoft Excel to obtain the $IC_{50}$ of the test compounds.

### 5.5.4. In vitro cytotoxicity assay

The anti-proliferative cytotoxic activities of target compounds were determined using a standard (MTT)-based colorimetric assay (Sigma). The tested cells were introduced into each well of a 96-well plate, with a density of 4000 cells/well. After 24 h, exponentially growing cells were exposed to the indicated compounds at final concentrations ranging from 1.0 to 32 μM. Controls were performed in which only culture media was added into wells containing cells. After 72 h incubation, 5 mg/ml MTT solution (20 μL/well) was added and cultured for 4 h, and then the supernatant was discarded and DMSO was added in (100 μL/well), respectively. The suspension was placed on micro-vibrator for 15 min and the absorbance (A) was measured at 570 nm by the Thermo Multiskan Spectrum. The results were obtained in one independent experiment run in triplicate.

## Acknowledgments

Acknowledgments are made to the National Natural Science Foundation of China (Grant Nos. 30801437 and 30772624). Specialized Research Fund for the Doctoral Program of Higher Education (20090096110003), and the National Major Science and Technology Project of China (Innovation and Development of New Drugs) (2008ZX09401-001, 2009ZX09501-003) for financial supports.

## References and notes

1. Lawrence, C. J.; Dawe, R. K.; Christie, K. R.; Cleveland, D. W.; Dawson, S. C.; Endow, S. A.; Goldstein, L. S.; Goodson, H. V.; Hirokawa, N.; Howard, J.; Malmberg, R. L.; McIntosh, J. R.; Miki, H.; Mitchison, T. J.; Okada, Y.; Reddy, A. S.; Saxton, W. M.; Schliwa, M.; Scholey, J. M.; Vale, R. D.; Walczak, C. E.; Wordeman, L. *J. Cell Biol.* **2004**, *167*, 19.
2. Mayer, T. U.; Kapoor, T. M.; Haggarty, S. J.; King, R. W.; Schreiber, S. L.; Mitchison, T. J. *Science* **1999**, *286*, 971.
3. Lad, L.; Luo, L.; Carson, J. D.; Wood, K. W.; Hartman, J. J.; Copeland, R. A.; Sakowicz, R. *Biochemistry* **2008**, *47*, 3576.
4. Sakowicz, R.; Finer, J. T.; Beraud, C.; Crompton, A.; Lewis, E.; Fritsch, A.; Lee, Y.; Mak, J.; Moody, R.; Turincio, R.; Chabala, J. C.; Gonzales, P.; Roth, S.; Weitman, S.; Wood, K. W. *Cancer Res.* **2004**, *64*, 3276.
5. Woessner, R.; Tunquist, B.; Lemieux, C.; Chlipala, E.; Jackinsky, S.; Dewolf, W., Jr.; Voegtli, W.; Cox, A.; Rana, S.; Lee, P.; Walker, D. *Anticancer Res.* **2009**, *29*, 4373.
6. Huszar, D.; Theoclitou, M. E.; Skolnik, J.; Herbst, R. *Cancer Metastasis Rev.* **2009**, *28*, 197.
7. Yang, L.; Jiang, C.; Liu, F.; You, Q. D.; Wu, W. T. *Biol. Pharm. Bull.* **2008**, *31*, 1397.
8. Garuti, L.; Roberti, M.; Bottegoni, G. *Curr. Med. Chem.* **2009**, *16*, 1949.
9. Bavetsias, V.; Sun, C.; Bouloc, N.; Reynisson, J.; Workman, P.; Linardopoulos, S.; McDonald, E. *Bioorg. Med. Chem. Lett.* **2007**, *17*, 6567.
10. Moriarty, K. J.; Koblish, H. K.; Garrabrant, T.; Maisuria, J.; Khalil, E.; Ali, F.; Petrounia, I. P.; Crysler, C. S.; Maroney, A. C.; Johnson, D. L.; Galemmo, R. A., Jr. *Bioorg. Med. Chem. Lett.* **2006**, *16*, 5778.
11. Harrington, E. A.; Bebbington, D.; Moore, J.; Rasmussen, R. K.; Ajose-Adeogun, A. O.; Nakayama, T.; Graham, J. A.; Demur, C.; Hercend, T.; Diu-Hercend, A.; Su, M.; Golec, J. M.; Miller, K. M. *Nat. Med.* **2004**, *10*, 262.
12. Young, M. A.; Shah, N. P.; Chao, L. H.; Seeliger, M.; Milanov, Z. V.; Biggs, W. H., 3rd; Treiber, D. K.; Patel, H. K.; Zarrinkar, P. P.; Lockhart, D. J.; Sawyers, C. L.; Kuriyan, J. *Cancer Res.* **2006**, *66*, 1007.
13. Giet, R.; Uzbekov, R.; Cubizolles, F.; Le Guellec, K.; Prigent, C. *J. Biol. Chem.* **1999**, *274*, 15005.
14. Liu, F.; You, Q. D.; Chen, Y. D. *Bioorg. Med. Chem. Lett.* **2007**, *17*, 722.
15. Jiang, C.; You, Q.; Liu, F.; Wu, W.; Guo, Q.; Chern, J.; Yang, L.; Chen, M. *Chem. Pharm. Bull. (Tokyo)* **2009**, *57*, 567.
16. Shaabani, A.; Rahmati, A.; Naderi, S. *Bioorg. Med. Chem. Lett.* **2005**, *15*, 5553.
17. Yao, C. S.; Lei, S.; Wang, C. H.; Yu, C. X.; Shao, Q. Q.; Tu, S. J. *Chinese J. Chem.* **2008**, *26*, 2107.
18. Ruan, X. Q.; You, Q. D.; Yang, L.; Wu, W. T. *Yao. Xue. Xue. Bao.* **2008**, *43*, 828.
19. Lewandowski, K.; Murer, P.; Svec, F.; Frechet, J. M. *J. Comb. Chem.* **1999**, *1*, 105.
20. Finer, J. T.; Bergnes, G.; Feng, B.; Smith, W. W.; Chabala, J. C.; Morgans, D. J. J. WO 0198278 A1, 2001.
21. Bavetsias, V.; McDonald, E.; Linardopoulos, S. WO 2007/072017 A2, 2007.
22. McDonnell, P. A.; Yanchunas, J.; Newitt, J. A.; Tao, L.; Kiefer, S. E.; Ortega, M.; Kut, S.; Burford, N.; Goldfarb, V.; Duke, G. J.; Shen, H.; Metzler, W.; Doyle, M.; Chen, Z.; Tarby, C.; Borzilleri, R.; Vaccaro, W.; Gottardis, M.; Lu, S.; Crews, D.; Kim, K.; Lombardo, L.; Roussell, D. L. *Anal. Biochem.* **2009**, *392*, 59.
23. Software-predicted lipophilicity of the compounds was calculated with the program accessible via internet (http://www.molinspiration.com).